to explain the influence of several factors, such as the bulk solution pH, solubility, and diffusivity, on the dissolution rate of the acids.

REFERENCES

(1) W. Nernst, *Z. Phys. Chem.*, **47**, 55 (1904).

(2) E. Brunner, *ibid.*, **47**, 56 (1904).

(3) C. V. King and J. S. Brodie, *J. Am. Chem. Soc.*, **59**, 1375 (1937).

(4) A. W. Hixson and S. Baum, *J. Ind. Eng. Chem.*, **36**, 528 (1944).

(5) W. I. Higuchi, E. Parrott, D. Wurster, and T. Higuchi, *J. Am. Pharm. Assoc., Sci. Ed.*, **47**, 376 (1958).

(6) W. I. Higuchi, E. Nelson, and J. G. Wagner, *J. Pharm. Sci.*, **53**, 333 (1964).

(7) W. E. Hamlin and W. I. Higuchi, *ibid.*, **55**, 205 (1966).

(8) A. Fick, *Ann. Phys.*, **94**, 59 (1855).

(9) W. H. Steinburg, H. H. Hutchins, P. G. Pick, and J. S. Lazer, *J. Pharm. Sci.*, **54**, 625 (1965).

(10) *Ibid.*, **54**, 761 (1965).

(11) A. Shah, *J. Pharm. Sci.*, **60**, 1564 (1971).

(12) J. H. Collett, J. A. Rees, and N. A. Dickinson, *J. Pharm. Pharmacol.*, **24**, 724 (1972).

(13) F. Underwood and D. Cadwallader, *J. Pharm. Sci.*, **67**, 1163 (1978).

(14) J. H. Wood, J. E. Syrato, and H. Letterman, *ibid.*, **54**, 1068 (1965).

(15) V. G. Levich, "Physico-chemical Hydrodynamics," Prentice-Hall, Englewood Cliffs, N.J., 1962.

(16) S. Prakongpan, A. H. Molokhia, K. H. Kwan, and W. I. Higuchi, *J. Pharm. Sci.*, **65**, 685 (1976).

(17) A. Tsuji, E. Nakashima, S. Hamano, and T. Yamana, *ibid.*, **67**, 1059 (1978).

(18) A. Goldberg, in "Dissolution Technology," L. J. Leeson and J. T. Carstensen, Eds., Industrial Pharmaceutical Technology Section, APhA Academy of Pharmaceutical Science, Washington, D.C., 1974.

(19) M. Gibaldi, in "The Theory and Practice of Industrial Pharmacy," L. Lachman, H. Lieberman, and J. Kanig, Eds., Lea & Febiger, Philadelphia, Pa., 1970, p. 246.

(20) B. Carnahan, H. A. Luther, and J. O. Wilkes, "Applied Numerical Methods," Wiley, New York, N.Y., 1969, p. 171.

(21) D. D. Perrin, D. R. Perrin, and W. Armarego, "Purification of Laboratory Chemicals," Pergamon, Oxford, England, 1966.

(22) R. Pakula, L. Pichnej, S. Spychala, and K. Butkiewicz, *Pol. J. Pharmacol. Pharm.*, **29**, 151 (1977).

(23) S. Spychala, K. Butkiewicz, R. Pakula, and L. Picknej, *ibid.*, **29**, 157 (1977).

(24) "Physical Pharmacy," A. N. Martin, J. Swarbrick, and A. Cammarata, Eds., Lea & Febiger, Philadelphia, Pa., 1969.

(25) E. R. Garrett and C. H. Won, *J. Pharm. Sci.*, **60**, 1801 (1971).

(26) S. Goto, W. Tseng, M. Kai, S. Aizawa, and S. Iguchi, *Yakuzaigaku*, **29**, 118 (1969).

(27) B. R. Hajratwala and J. E. Dawson, *J. Pharm. Sci.*, **66**, 27 (1977).

(28) E. Pawetczyk and B. Knitter, *Pharmazie*, **33**, 586 (1978).

(29) H. Nogami, T. Nagai, and A. Suzuki, *Chem. Pharm. Bull.*, **14**, 329 (1966).

(30) A. H. Goldberg and W. I. Higuchi, *J. Pharm. Sci.*, **57**, 1583 (1968).

(31) G. L. Flynn, S. H. Yalkowsky, and T. J. Roseman, *ibid.*, **63**, 479 (1974).

(32) R. C. Reid and T. K. Sherwood, "Properties of Gases and Liquids," McGraw-Hill, New York, N.Y., 1966.

(33) "International Critical Tables of Numerical Data, Physics, Chemistry and Technology," McGraw-Hill, New York, N.Y., 1926.

(34) S. Dayal, T. Higuchi, and I. Pitman, *J. Pharm. Sci.*, **61**, 695 (1972).

(35) R. H. Stokes, *J. Am. Chem. Soc.*, **72**, 2243 (1950).

(36) S. B. Tuwiner, "Diffusion and Membrane Technology," Reinhold, New York, N.Y., 1962, p. 378.

(37) T. Erdey-Grûz, "Transport Phenomena in Aqueous Solutions," Wiley, New York, N.Y., 1974.

(38) D. Eisenberg and W. Kauzman, "Structure and Properties of Water," Oxford University Press, New York, N.Y., 1969, pp. 217–224.

(39) D. P. Gregory and A. C. Riddiford, *J. Chem. Soc.*, **1956**, 3756.

ACKNOWLEDGMENTS

Adapted in part from a dissertation submitted by K. G. Mooney to the University of Kansas in partial fulfillment of the Doctor of Philosophy degree requirements.

Supported by Grant GM22357 from the National Institutes of Health.

Dissolution Kinetics of Carboxylic Acids II: Effect of Buffers

K. G. MOONEY *, M. A. MINTUN ‡, K. J. HIMMELSTEIN, and V. J. STELLA ˣ

Received March 24, 1980, from the *Departments of Pharmaceutical Chemistry and Chemical and Petroleum Engineering, University of Kansas, Lawrence, KS 66045.* Accepted for publication July 3, 1980.

*Present address: Boehringer Ingelheim, Ridgefield, CT 06877. ‡Present address: Washington University, St. Louis, MO 63110.

Abstract □ The dissolution behavior of 2-naphthoic acid from rotating compressed disks into aqueous buffered solutions of constant ionic strength (μ = 0.5 with potassium chloride) at 25° was investigated. A model was developed for the flux of a solid monoprotic carboxylic acid in aqueous buffered solutions as a function of the solution pH and the physicochemical properties of the buffer. The model assumes a diffusion layer-controlled mass transport process and a simple, instantaneously established reaction equilibrium between all reactive species (acids and bases) across the diffusion layer. Using intrinsic solubilities, pKa values, and diffusion coefficients, the model accurately predicts the dissolution of 2-naphthoic acid as a function of the bulk solution composition. The concentration profiles of all species across the diffusion layer are generated for each buffer concentration and bulk solution pH, including the pH profile within the microclimate of the diffusion layer and the pH at the solid–solution boundary.

Keyphrases □ Carboxylic acids—dissolution kinetics, effect of buffers □ Dissolution kinetics—carboxylic acids, effect of buffers □ Buffers—effect on dissolution kinetics of carboxylic acids

The objective of this investigation was to determine experimentally the effect of buffers on the dissolution of 2-naphthoic acid from a constant surface area pellet under controlled ionic strength (μ = 0.5 with potassium chloride), temperature (25°), and pH conditions (pH-stat). A model, an extension of one described previously (1), also was de-

0022-3549/81/0100-0022$01.00/0

© 1981, American Pharmaceutical Association

veloped that predicts the effects of solution pH and the physicochemical properties of the buffer on the dissolution of this monoprotic carboxylic acid. The model adequately predicts fluxes and the concentration profiles of all species within a postulated diffusion layer as a function of the bulk solution pH (pH_{bulk}) and the total buffer concentration. The results emphasize the importance of the buffer base concentration and the pKa value of the conjugate acid of the buffer on dissolution rates, but they deemphasize the direct involvement and importance of pH_{bulk}.

Alkaline compounds or buffers have been included in commercial tablet formulations of several acidic drugs that undergo dissolution rate-limited absorption from conventional tablets. The concept embodied in these buffered formulations is the prevention of GI irritation caused by some acidic drugs and/or the provision of a basic pH microenvironment within the diffusion layer around the dissolving acid particles to promote dissolution (2–4). Nelson (5, 6) first approached the rationale for buffered tablet formulations when he measured the dissolution rates of several solid acidic drugs in aqueous media containing various buffers at several pH values. The mechanism of this process was studied in detail by Higuchi and coworkers (7, 8). The results presented here support the use of buffered dosage forms to promote the dissolution of poorly soluble carboxylic acids.

THEORETICAL

A model for the dissolution of an acid into an aqueous buffered medium should consider not only the diffusion layer reaction of the acid with water and hydroxide ion but also the reaction of the acid with the base component of the buffer. Hence, the number of possible chemical reactions that occur in the diffusion layer is increased because the buffer consists of a conjugate acid–base pair, which is assumed to be in rapid equilibrium with the other reactants and products.

It is assumed that the addition of buffer to the bulk solution does not change the constraints and assumptions of the previously described model (1), *i.e.*, that the dissolution of the acid (HA) into the aqueous buffer solution occurs *via* a diffusion layer-controlled process across a boundary layer of thickness h as defined by the Levich rotating-disk model (9). A constant diffusion layer thickness, calculated on the basis of the diffusivity of the acid (D_{HA}) and regardless of the diffusivities of other species, is assumed. The limitations of this assumption were discussed earlier (1).

Within this boundary layer, all concentration gradients of the reactants and products exist as a result of diffusion and instantaneous chemical reaction between the dissolving solute and the incoming base from the bulk solution. The concentration of undissociated carboxylic acid at the solid–liquid surface ($X = 0$, where X is the distance from the solid–liquid interface) always is defined by the intrinsic solubility of the acid $[HA]_0$. The bulk solution is regarded as a homogeneous mixture with no concentration gradients, and initial rates are assumed.

An additional experimental constraint is that the buffering compounds considered contain only one ionizable group. Polyprotic or polybasic compounds also may be considered in the model; however, they obviously would complicate the situation.

Figure 1 is a schematic diagram of this system. Hydroxide ion (OH^-) and the buffer base (B) may diffuse into the diffusion layer from the bulk solution and react with the carboxylic acid (HA) which is diffusing out. The products, also diffusing out, are the conjugate acid of the buffer (BH^+), the acid anion (A^-), and the hydrogen ion (H^+). The water concentration is ignored since its concentration does not change significantly as a result of these reactions.

Consider the chemical reactions within the diffusion layer as shown by Fig. 1 (Schemes I–VI).

$$H^+ + OH^- \rightleftharpoons H_2O$$
Scheme I

$$HA \overset{K_a^A}{\rightleftharpoons} H^+ + A^-$$
Scheme II

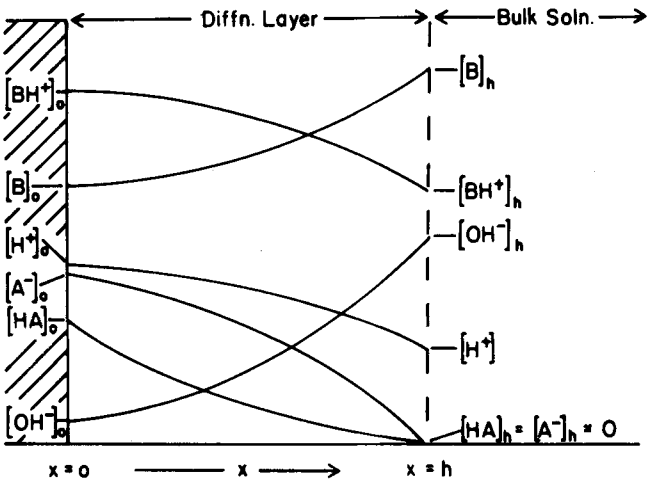

Figure 1—*Diagrammatic representation of a solid carboxylic acid, HA, dissolving into a reactive medium containing hydroxide ion and buffer components B and BH^+ with a Nernst diffusion layer existing between the solid and the bulk solution. Sink conditions exist in the bulk solution, and the products, BH^+, A^-, and H^+, diffuse out of the diffusion layer at a rate determined by their chemical reactivity and diffusivity.*

$$HA + OH^- \overset{K_1^*}{\rightleftharpoons} H_2O + A^-$$
Scheme III

$$HA + B \overset{K_2}{\rightleftharpoons} BH^+ + A^-$$
Scheme IV

$$BH^+ \overset{K_a^B}{\rightleftharpoons} H^+ + B$$
Scheme V

$$BH^+ + OH^- \overset{K_3^*}{\rightleftharpoons} H_2O + B$$
Scheme VI

These equilibria are described by:

$$K_w = [H^+][OH^-] \quad \text{(Eq. 1)}$$

$$K_a^A = \frac{[H^+][A^-]}{[HA]} \quad \text{(Eq. 2)}$$

$$K_1^*/[H_2O] = K_1 = \frac{[A^-]}{[HA][OH^-]} = \frac{1}{K_0^A} \quad \text{(Eq. 3)}$$

$$K_2 = \frac{[BH^+][A^-]}{[HA][B]} = \frac{K_a^A}{K_a^B} \quad \text{(Eq. 4)}$$

$$K_a^B = \frac{[H^+][B]}{[BH^+]} \quad \text{(Eq. 5)}$$

$$K_3^*/[H_2O] = K_3 = \frac{[B]}{[BH^+][OH^-]} \quad \text{(Eq. 6)}$$

For the diffusion and simultaneous chemical reaction of the individual species at steady state within the diffusion layer, Fick's laws may be applied to each species as discussed previously (1). Therefore:

$$\frac{\delta[HA]}{\delta t} = D_{HA}\frac{\delta^2[HA]}{\delta X^2} + \phi_1 = 0 \quad \text{(Eq. 7)}$$

$$\frac{\delta[A^-]}{\delta t} = D_A\frac{\delta^2[A^-]}{\delta X^2} + \phi_2 = 0 \quad \text{(Eq. 8)}$$

$$\frac{\delta[H^+]}{\delta t} = D_H\frac{\delta^2[H^+]}{\delta X^2} + \phi_3 = 0 \quad \text{(Eq. 9)}$$

$$\frac{\delta[OH^-]}{\delta t} = D_{OH}\frac{\delta^2[OH^-]}{\delta X^2} + \phi_4 = 0 \quad \text{(Eq. 10)}$$

$$\frac{\delta[B]}{\delta t} = D_B\frac{\delta^2[B]}{\delta X^2} + \phi_5 = 0 \quad \text{(Eq. 11)}$$

$$\frac{\delta[BH^+]}{\delta t} = D_{BH}\frac{\delta^2[BH^+]}{\delta X^2} + \phi_6 = 0 \quad \text{(Eq. 12)}$$

where $[N]$ represents the concentration of species N, t is time, X is distance, and D_N is the diffusivity of species N. Each equation states that the rate of change in the concentration of N with respect to time in the diffusion layer (here it is zero since steady-state conditions are assumed) is composed of a diffusional term (Fick's second law) and a chemical reaction term for the species N.

By observing which species react together to form particular products, a comprehensive set of species balance equations accounting for the chemical reaction may be established. Whenever a change in the flux of one species occurs due to a chemical reaction within the film, it also must be reflected by corresponding changes in the reactants and products as defined by the equilibria in Schemes I–VI. From these relationships, the following diffusion layer mass balance can be written:

$$\Delta(\text{flux } OH^- \text{ in}) + \Delta(\text{flux B in}) = \Delta(\text{flux HA out}) + \Delta(\text{flux } H^+ \text{ out}) \quad \text{(Eq. 13)}$$

Equation 13 states that the rates of change of the flux of reactants into the film, OH^- and B, must equal those of the reactants coming out of the film, HA and H^+; BH^+ and A^- are considered because any changes in B or HA will reflect changes in their conjugate species. Therefore:

$$D_{OH}\frac{d^2[OH^-]}{dX^2} + D_B\frac{d^2[B]}{dX^2} = D_{HA}\frac{d^2[HA]}{dX^2} + D_H\frac{d^2[H^+]}{dX^2} \quad \text{(Eq. 14)}$$

From species balance considerations, the chemical reaction terms ϕ_1, ϕ_3, ϕ_4, and ϕ_5 from Eqs. 7–12 are represented by:

$$\phi_4 + \phi_5 = \phi_1 + \phi_3 \quad \text{(Eq. 15)}$$

Any change in HA and B due to reaction automatically represents a change in their conjugate species, A^- and BH^+. This is represented by:

$$D_{HA}\frac{d^2[HA]}{dX^2} = -\left(D_A\frac{d^2[A^-]}{dX^2}\right) \quad \text{(Eq. 16)}$$

$$D_B\frac{d^2[B]}{dX^2} = -\left(D_{BH}\frac{d^2[BH^+]}{dX^2}\right) \quad \text{(Eq. 17)}$$

Therefore, $\phi_1 = -\phi_2$ and $\phi_5 = -\phi_6$.

Equations 14, 16, and 17 are three second-order differential equations. When integrated with respect to X, they yield:

$$D_{HA}\frac{d[HA]}{dX} = D_{OH}\frac{d[OH^-]}{dX} + D_B\frac{d[B]}{dX} - D_H\frac{d[H^+]}{dX} + C_1 \quad \text{(Eq. 18)}$$

$$D_{HA}\frac{d[HA]}{dX} = -\left(D_A\frac{d[A^-]}{dX}\right) + C_2 \quad \text{(Eq. 19)}$$

$$D_B\frac{d[B]}{dX} = -\left(D_{BH}\frac{d[BH^+]}{dX}\right) + C_3 \quad \text{(Eq. 20)}$$

where C_1, C_2, and C_3 are constants of integration. If mass balance considerations are included, simplification of Eqs. 18–20 is possible because A^- is a product of the reaction between HA and the combination of B, OH^-, and H_2O. However, B and OH^- also react with H^+ in the diffusion layer. Therefore, the following identities result:

$$\Sigma\,(\text{flux of reactants in}) = (\text{flux } A^- \text{ out}) - (\text{flux } H^+ \text{ out}) \quad \text{(Eq. 21)}$$

or:

$$\Sigma\,(\text{flux of reactants in}) = \left(D_{OH}\frac{d[OH^-]}{dX} + D_B\frac{d[B]}{dX}\right) \quad \text{(Eq. 22)}$$

Remembering that fluxes into the film have positive slopes and that:

$$\text{flux } A^- \text{ out} = -\left(D_A\frac{d[A^-]}{dX}\right) \quad \text{(Eq. 23)}$$

and:

$$\text{flux } H^+ \text{ out} = -\left(D_H\frac{d[H^+]}{dX}\right) \quad \text{(Eq. 24)}$$

yields:

$$D_{OH}\frac{d[OH^-]}{dX} + D_B\frac{d[B]}{dX} = D_H\frac{d[H^+]}{dX} - D_A\frac{d[A^-]}{dX} \quad \text{(Eq. 25)}$$

From Eqs. 18 and 19, it can be seen that consistency is preserved only when $C_2 = C_1$. Therefore, Eq. 19 becomes:

$$D_{HA}\frac{d[HA]}{dX} = -\left(D_A\frac{d[A^-]}{dX}\right) + C_1 \quad \text{(Eq. 26)}$$

Further simplification may be made by substituting Eq. 20 into Eq. 18 and rearranging:

$$D_{HA}\frac{d[HA]}{dX} = C_1 + C_3 + D_{OH}\frac{d[OH^-]}{dX} - D_H\frac{d[H^+]}{dX} - D_{BH}\frac{d[BH^+]}{dX} \quad \text{(Eq. 27)}$$

Equation 26 is substituted into Eq. 27 to obtain:

$$-\left(D_A\frac{d[A^-]}{dX}\right) = D_{OH}\frac{d[OH^-]}{dX} - D_H\frac{d[H^+]}{dX} - D_{BH}\frac{d[BH^+]}{dX} + C_3 \quad \text{(Eq. 28)}$$

Consider the reactions involving A^- separately. For the reaction shown in Scheme VII (Equilibrium a):

$$HA + H_2O \rightleftharpoons A^- + H_3O^+ \text{ (where } H_3O^+ = H^+)$$

Scheme VII

$$(\text{flux } A^- \text{ out})_a = (\text{flux } H^+ \text{ out}) \quad \text{(Eq. 29)}$$

or:

$$-\left(D_A\frac{d[A^-]}{dX}\right)_a = -\left(D_H\frac{d[H^+]}{dX}\right) \quad \text{(Eq. 30)}$$

For the reaction shown in Scheme III (Equilibrium b):

$$(\text{flux } A^- \text{ out})_b = (\text{flux } OH^- \text{ in}) \quad \text{(Eq. 31)}$$

or:

$$-\left(D_A\frac{d[A^-]}{dX}\right)_b = \left(D_{OH}\frac{d[OH^-]}{dX}\right) \quad \text{(Eq. 32)}$$

For the reaction shown in Scheme IV (Equilibrium c):

$$(\text{flux } A^- \text{ out})_c = (\text{flux } BH^+ \text{ out}) \quad \text{(Eq. 33)}$$

or:

$$-\left(D_A\frac{d[A^-]}{dX}\right)_c = -\left(D_{BH}\frac{d[BH^+]}{dX}\right) \quad \text{(Eq. 34)}$$

Hence, summing up the contributions of the three equilibria (a–c) in the diffusion layer:

$$\Sigma - \left(D_A\frac{d[A^-]}{dX}\right) = D_{OH}\frac{d[OH^-]}{dX} - D_H\frac{d[H^+]}{dX} - D_{BH}\frac{d[BH^+]}{dX} \quad \text{(Eq. 35)}$$

By comparing Eq. 35 to Eq. 28, it is seen that $C_3 = 0$. Equation 20 now becomes:

$$D_B\frac{d[B]}{dX} = -\left(D_{BH}\frac{d[BH^+]}{dX}\right) \quad \text{(Eq. 36)}$$

By integrating Eqs. 18, 26, and 36, linear equations are obtained in X:

$$D_{HA}[HA] = D_{OH}[OH^-] + D_B[B] - D_H[H^+] + C_1X + T_1 \quad \text{(Eq. 37)}$$

$$D_{HA}[HA] = -D_A[A^-] + C_1X + T_2 \quad \text{(Eq. 38)}$$

$$D_B[B] = -D_{BH}[BH^+] + T_3 \quad \text{(Eq. 39)}$$

where T_1, T_2, and T_3 are additional constants of integration.

Application of Boundary Conditions—To evaluate Eqs. 37–39, the following boundary conditions must be applied.

At $X = 0$:

$[HA] = [HA]_0$ (known)
$[A^-] = [A^-]_0$ (unknown)
$[H^+] = [H^+]_0$ (unknown)
$[OH^-] = [OH^-]_0$ (unknown)
$[B] = [B]_0$ (unknown)
$[BH^+] = [BH^+]_0$ (unknown)

At $X = h$:

$[HA] = [HA]_h \simeq 0$
$[A^-] = [A^-]_h \simeq 0$
$[H^+] = [H^+]_h$ (given)

$[OH^-] = [OH^-]_h$ (given)
$[B] = [B]_h$ (given)
$[BH^+] = [BH^+]_h$ (given)

Both $[HA]_h$ and $[A^-]_h$ are zero under sink conditions. Other terms (C_1, T_1, T_2, and T_3) are unknown. Applying the boundary conditions to Eqs. 37–39 at $X = 0$ results in:

$$D_{HA}[HA]_0 = D_{OH}[OH^-]_0 + D_B[B]_0 - D_H[H^+]_0 + T_1 \quad \text{(Eq. 40)}$$

$$D_{HA}[HA]_0 = -D_A[A^-]_0 + T_3 \quad \text{(Eq. 41)}$$

$$D_B[B]_0 = -D_{BH}[BH^+] + T_3 \quad \text{(Eq. 42)}$$

and at $X = h$:

$$D_H[H^+]_h = D_{OH}[OH^-]_h + D_B[B]_h + C_1h + T_1 \quad \text{(Eq. 43)}$$

$$C_1h = -T_2 \quad \text{(Eq. 44)}$$

$$D_B[B]_h = -D_{BH}[BH^+]_h + T_3 \quad \text{(Eq. 45)}$$

There are nine unknowns in these equations, providing that $[HA]_0$, the diffusivities of all species, and h are known. To calculate the unknowns, three more equations are required. These are provided by the equilibrium constants given in Eqs. 1, 2, and 5.

There are now nine equations and nine unknowns. Successive substitution may be used to reduce these equations to one equation where a single unknown may be solved for. A brief summary for the solution of $[H^+]_0$ is given here.

Equation 43 is subtracted from Eq. 40 to give:

$$D_{HA}[HA]_0 = D_{OH}([OH^-]_0 - [OH^-]_h) + D_B([B]_0 - [B]_h) + D_H([H^+]_h - [H^+]_0) - C_1h \quad \text{(Eq. 46)}$$

Equation 46 was derived to eliminate T_1. Now $[A^-]_0$ is substituted for in Eq. 41 using Eq. 2, and T_2 is eliminated by using Eq. 44:

$$D_{HA}[HA]_0 = -D_A\frac{K_a^A[HA]_0}{[H^+]_0} - C_1h \quad \text{(Eq. 47)}$$

Equation 47 may now be equated to Eq. 46 to cancel C_1h. Substituting for $[OH^-]_0$ also results in:

$$-D_A\frac{K_a^A[HA]_0}{[H^+]_0} = \frac{D_{OH}K_w}{[H^+]_0} + D_B[B]_0 - D_H[H^+]_0 - (D_{OH}[OH^-]_h + D_B[B]_h - D_H[H^+]_h) \quad \text{(Eq. 48)}$$

To obtain $[B]_0$ in terms of $[H^+]_0$, Eqs. 42, 45, and 5 must be used:

$$T_3 = D_B[B]_0 + D_{BH}[BH^+]_0 = D_B[B]_h + D_{BH}[BH^+]_h \quad \text{(Eq. 49)}$$

Substituting for $[BH^+]_0$:

$$[B]_0 = K_a^B\left[\frac{D_B[B]_h + D_{BH}[BH^+]_h}{D_BK_a^B + D_{BH}[H^+]_0}\right] \quad \text{(Eq. 50)}$$

Equation 50 may be used to substitute for $[B]_0$ in Eq. 48 and, hence, reduce it to one with a single unknown, $[H^+]_0$. After cross-multiplication and rearrangement:

$$p[H^+]_0^3 + q[H^+]_0^2 + r[H^+]_0 + s = 0 \quad \text{(Eq. 51)}$$

where:

$p = D_HD_{BH}$
$q = D_HD_BK_a^B + D_{BH}a$
$r = D_BK_a^B(a - b) - D_AD_{BH}K_a^A[HA]_0 - D_{OH}D_{BH}K_w$
$s = -D_AD_BK_a^AK_a^B[HA]_0 - D_{OH}K_wK_a^BD_B$
$a = D_{OH}[OH^-]_h + D_B[B]_h - D_H[H^+]_h$
$b = D_B[B]_h + D_{BH}[BH^+]_h$ (also $= T_3$)

Equation 51 may be solved by the method of Newton (10). Thus, for any given conditions in the bulk solution of $[H^+]_h$, $[OH^-]_h$, $[B]_h$, and $[BH^+]_h$, $[H^+]_0$ may be determined. Once this value is obtained, the other unknowns may be successively calculated from the preceding equations. Equation 51, together with its related questions, may be solved readily using a digital computer[1].

Expression for the Total Acid Flux—Equation 46 may be rearranged to give an expression for the integration constant C_1; C_1 represents the negative sum of the individual fluxes across the diffusion layer and, therefore, is the negative of the total acid flux at $X = 0$ or the acid dissolution rate:

$$C_1 = -J^{total} = -1/h[D_{HA}[HA]_0 + D_H([H^+]_0 - [H^+]_h) + D_{OH}([OH^-]_h - [OH^-]_0) + D_B([B]_h - [B]_0)] \quad \text{(Eq. 52)}$$

or:

$$C_1 = -J^{total} = -(J_{HA} + J_H + J_{OH} + J_B) \quad \text{(Eq. 53)}$$

where J_N is the flux of species N.

Therefore, by using the values of $[H^+]_0$, $[B]_0$, and $[OH^-]_0$ calculated from the preceding equations, the total flux of acid at any bulk solution pH and buffer concentration also may be calculated. Again, this problem may be included in a comprehensive computer program[1] for application to various bulk solution pH and buffer concentrations.

Evaluation of Concentration Profiles across Diffusion Layer—Using the Levich (9) diffusion layer thickness for a rotating disk, Eqs. 37–39 may be solved simultaneously with Eqs. 1, 2, and 5 to give the concentrations of a particular species at any point, X, in the diffusion layer. The substitutions required in reducing the numerous equations to one equation with a single unknown are similar to those already described, except that [HA] also must be expressed as a function of the given unknown solved. This may be done by using Eqs. 2 and 38:

$$[HA] = [H^+]\left(\frac{C_1X + T_2}{D_{HA}[H^+] + D_AK_a^A}\right) \quad \text{(Eq. 54)}$$

Now [HA] can be substituted for Eq. 37 along with a similar expression for [B], which is derived from Eqs. 39 and 5:

$$[B] = \left(\frac{K_a^BT_3}{D_BK_a^B + D_{BH}[H^+]}\right) \quad \text{(Eq. 55)}$$

Equation 37 now reads:

$$D_{HA}[H^+]\left(\frac{C_1X + T_2}{D_{HA}[H^+] + D_AK_a^A}\right) = \frac{D_{OH}K_w}{[H^+]} - D_H[H^+] + D_B\left(\frac{K_a^BT_3}{D_BK_a^B + D_{BH}[H^+]}\right) + C_1X + T_1 \quad \text{(Eq. 56)}$$

Since C_1, T_2, and T_3 already are known for given bulk solution conditions and X is given, $[H^+]$ now is the only unknown. By algebraic rearrangement, cross-multiplication, and reduction, a quartic equation in $[H^+]$ results in the form of:

$$A[H^+]^4 + B[H^+]^3 + C[H^+]^2 + E[H^+] + F = 0 \quad \text{(Eq. 57)}$$

where:

$A = D_Hn$
$B = n(T_2 - T_1) + D_Ht$
$C = D_BD_{HA}K_a^B(C_1X + T_2 - T_3) - t(C_1X + T_1) - D_{OH}K_wn + D_Hp$
$E = -D_{OH}K_wt - p(C_1X + T_1 + T_3)$
$F = -pK_wD_{OH}$
$n = D_{HA}D_{BH}$
$t = D_{HA}D_BK_a^B + D_AD_{BH}K_a^A$
$p = D_AD_BK_a^AK_a^B$

Equation 57 can be solved by using Newton's method (10). Having obtained $[H^+]$ at any point X in the film, the concentrations of the other species may be determined. If this calculation is performed at several points in the diffusion layer, then a concentration profile across this layer is described.

EXPERIMENTAL

Materials—2-Naphthoic acid was from the same source as that used previously (1). Imidazole[2], acetic acid[3], sodium acetate[3] (trihydrate), morpholine[4], and potassium chloride[3] were reagent grade and were used as supplied. Hydrochloric acid[5] and sodium hydroxide[5] were obtained as standardized 1.0 *M* solutions.

Determination of Dissolution Rates—The apparatus for determining the dissolution rates of 2-naphthoic acid was described previously (1). In each determination, the pH-stat was used to maintain the bulk

[1] Honeywell model 66/60. A copy of the procedure and program can be obtained from V. J. Stella.

[2] Sigma Chemical Co., St. Louis, Mo.
[3] Mallinckrodt Chemicals.
[4] Matheson, Coleman and Bell.
[5] Fisher Scientific Co., Fair Lawn, N.J.

Table I—Experimental pKa Values, Estimated Percentage Purity, and Literature Thermodynamic pKa Values for Imidazole, Morpholine, and Acetic Acid

Compound	pKa (±*SD*)[a] at μ = 0.5 (Potassium Chloride) and 25° (±0.1°)	pKa (Thermodynamic) at 25° in Water	Estimated Purity, %
Imidazole	7.17 (±0.01)	6.91[b]	102.24
Morpholine	8.75 (±0.02)	8.70[c]	97.92
Acetic acid	4.60[b]	4.75[b]	—

[a] The standard deviation from at least three determinations. [b] Obtained or estimated from data in Ref. 11. [c] From Ref. 12.

Table II—Estimated and Literature Values for the Diffusivities of Imidazole, Morpholine, and Acetic Acid, Used as Buffering Agents in the Study of 2-Naphthoic Acid Dissolution at μ = 0.5 with Potassium Chloride and 25°

Compound	Molecular Weight	Diffusivity, $cm^2/sec \times 10^6$	
		Calculated[a]	Literature (Ref.)
Imidazole	68	8.20[b]	—
Morpholine	87	7.00[c]	—
Acetic acid	79	8.84[d]	12.1[e] (14) 12.0[e] (15) 8.8[f] (16)

[a] Using Stokes–Einstein equation (1). [b] By direct comparison with 2-naphthoic acid using the Stokes–Einstein equation. [c] A molar volume of 87 ml/mole was used, assuming the density to be 1.0 at 25°. [d] A molar volume of 38.3 ml/mole was used from Ref. 14 at 25°. [e] Extrapolated to zero acetic acid concentration (μm = 0) at 25° in water. [f] In water at 20°; other conditions not stipulated.

solution pH using 0.01–0.1 *M* NaOH, regardless of the buffer capacity of the buffer solution used.

When imidazole and morpholine were used as buffers, it was convenient to measure the absorbance of 2-naphthoic acid in the solution at 281 nm rather than at the more analytically sensitive region of 230–237 nm because the absorbance of imidazole interfered in the latter range. Furthermore, dissolution became so rapid at high buffer concentrations that the absorbance of the resulting solution quickly exceeded the range obeying the Beer–Lambert law. In acetate buffers, measurement of the dissolution rate was performed at 231 or 281 nm, depending on the buffer concentration and the pH of the dissolution medium.

In all cases, the media were adjusted to the same ionic strength (μ = 0.5) using potassium chloride. A wide range of total buffer concentrations was studied. Immediately prior to a dissolution run, the solution pH was accurately adjusted with concentrated hydrochloric acid or sodium hydroxide, and the solution then was thermally equilibrated to 25° (±0.1°). In each case, the solution used for the dissolution served as its own reference in the spectrophotometer.

2-Naphthoic acid was chosen for the investigation of buffer effects because of its intermediate aqueous solubility in the three acids used previously (1), its chemical stability, and its amenability to spectrophotometric analysis. The disks of 2-naphthoic acid were prepared as described previously (1), and all dissolution experiments were performed at disk rotation speeds of 450 rpm. Sink conditions were maintained throughout, as observed from the linear dissolution plots obtained.

Determination of Buffer pKa Values—The pKa values of imidazole and morpholine were measured at μ = 0.5 (potassium chloride) and 25° (±0.1°) using potentiometric titrimetry. The pKa value of acetic acid was obtained by estimation by the method of Butler (10).

RESULTS AND DISCUSSION

The pKa values of imidazole and morpholine determined experimentally, the thermodynamic pKa values, and the estimated purity of the titrated buffers are given in Table I together with the estimated pKa for acetic acid at an ionic strength of 0.5.

Diffusion Coefficients for Various Species—Since the aqueous diffusion coefficients of the buffer species were not measured, literature values and estimations based on the Stokes–Einstein equation (1, 13) were used. They are summarized in Table II. The literature diffusivities (where available) differed significantly from the calculated values at 25°. The aqueous diffusivities of all weak electrolytes are strongly affected by the ionic strength of the solution and the concentration of the weak electrolyte itself. In the case of acetic acid, diffusivity values decline almost linearly with an increase in the acid concentration in the aqueous medium (14). Similar effects were noted on the diffusivity of ions in solutions of mixed electrolytes (17). Both phenomena are due to an alteration of the thermodynamic activity coefficient of the diffusant. Hence, the actual diffusivities of imidazole, morpholine, and acetic acid at μ = 0.5 (potassium chloride) and 25° in water are likely to be lower than those measured under the same conditions with μ approaching zero (infinite dilution). For this reason, the diffusivities calculated from the Stokes–Einstein equation as described previously (1) were used since these values are lower than those quoted in the literature for diffusivity in water at 25°.

Initial Dissolution Rate of 2-Naphthoic Acid as a Function of Bulk Solution Buffer Concentration and pH—The model discussed under *Theoretical* was tested over a wide range of bulk solution pH values and total buffer concentrations using acetic acid, imidazole, and morpholine buffers. Experimentally determined initial dissolution rates for 2-naphthoic acid (J_{obs}) are given in Tables III–V together with the corresponding interfacial pH (pH_0) calculated from Eq. 51 and theoretical initial dissolution rates (J_{theor}) calculated from Eq. 52. Figures 2–4 show J_{obs} and J_{theor} *versus* the total bulk solution buffer concentration for the three buffers used.

The agreement between the observed and predicted initial dissolution rates was good over wide ranges of bulk solution buffer concentrations and pH bulk values for all three buffer systems. The data from the acetate buffers are of particular interest since the acetic acid pKa (4.60) is similar to that of 2-naphthoic acid (4.02) and, therefore, the equilibrium constant for the reaction between the two is relatively low (K_2 = 3.8). Thus, the degree of catalysis of the dissolution of 2-naphthoic acid by acetate anion diffusing into the aqueous diffusion layer and reacting with dissolving acid is expected to be relatively small compared to that resulting from

Table III—Comparison of the Observed (J_{obs}) and Theoretical (J_{theor}) Initial Dissolution Rates of 2-Naphthoic Acid in Varying Bulk Solution Acetate Buffer Concentrations at pH_{bulk} 4.50, 5.00, and 6.00 (μ = 0.5 with Potassium Chloride and 25°)[a]

Total Bulk Solution Concentration of Acetate, *M*	pH_{bulk} 4.50			pH_{bulk} 5.00			pH_{bulk} 6.00		
	J_{obs}, moles/cm^2/sec $\times 10^9$	J_{theor}, moles/cm^2/sec $\times 10^9$	pH_0	J_{obs}, moles/cm^2/sec $\times 10^9$	J_{theor}, moles/cm^2/sec $\times 10^9$	pH_0	J_{obs}, moles/cm^2/sec $\times 10^9$	J_{theor}, moles/cm^2/sec $\times 10^9$	pH_0
0.0	1.03	0.95	4.15	1.19	1.07	4.24	1.33	1.13	4.28
0.00025	1.10	1.01	4.20	—	1.27	4.35	—	1.49	4.45
0.0005	1.24	1.07	4.24	—	1.46	4.44	—	1 83	4.57
0.001	1.39	1.17	4.30	—	1.75	4.54	—	2.41	4.72
0.0025	1.41	1.32	4.38	2.50	2.32	4.70	3.74	3.67	4.93
0.005	—	1.43	4.42	3.10	2.81	4.79	5.20	5.10	5.09
0.01	1.63	1.51	4.46	3.45	3.27	4.87	7.11	7.07	5.24
0.025	—	1.57	4.48	3.88	3.75	4.94	10.67	10.64	5.42
0.05	—	1.60	4.49	4.16	3.97	4.97	13.52	14.17	5.55
0.075	—	1.60	4.49	4.14	4.06	4.98	15.95	16.55	5.62
0.10	1.70	1.61	4.50	4.10	4.11	4.98	18.53	18.23	5.67

[a] J_{theor} was calculated from Eq. 52. The estimated interfacial pH (pH_0) for each condition was determined from Eq. 51. The rates were measured from a disk rotating at 450 rpm. Each J_{obs} value is the mean from at least two runs.

Table IV—Comparison of the Observed (J_{obs}) and Theoretical (J_{theor}) Initial Dissolution Rates of 2-Naphthoic Acid from a Disk Rotating at 450 rpm into Varying Bulk Solution Concentrations of Imidazole Buffer at pH_{bulk} 6.00, 7.00, and 8.00 (μ = 0.5 with Potassium Chloride and 25°) [a]

Total Bulk Solution Concentration of Imidazole, M	pH_{bulk} 6.00			pH_{bulk} 7.00			pH_{bulk} 8.00		
	J_{obs}, moles/cm²/sec × 10^9	J_{theor}, moles/cm²/sec × 10^9	pH_0	J_{obs}, moles/cm²/sec × 10^9	J_{theor}, moles/cm²/sec × 10^9	pH_0	J_{obs}, moles/cm²/sec × 10^9	J_{theor}, moles/cm²/sec × 10^9	pH_0
0.0	1.33	1.13	4.28	1.38	1.14	4.28	1.36	1.15	4.29
0.0001	—	1.14	4.28	1.58	1.23	4.33	—	1.35	4.39
0.0005	—	1.20	4.31	2.31	1.66	4.51	—	2.47	4.73
0.001	—	1.27	4.35	2.89	2.33	4.70	—	4.13	4.98
0.005	—	1.98	4.61	9.84	8.50	5.32	20.84	17.80	5.65
0.01	3.72	3.02	4.83	17.44	15.98	5.61	38.94	34.06	5.94
0.015	—	4.06	4.98	24.87	23.02	5.77	—	49.43	6.10
0.0175	—	4.57	5.03	—	26.39	5.83	62.55	56.81	6.16
0.025	6.66	6.01	5.16	41.09	35.96	5.96	84.45	77.92	6.30
0.0375	—	8.17	5.30	—	50.35	6.11	108.96	110.21	6.45
0.04	—	8.57	5.33	56.51	53.03	6.13	—	116.30	6.48
0.05	12.12	10.07	5.40	67.67	63.16	6.21	128.88	139.63	6.56
0.0625	—	11.68	5.47	—	74.70	6.28	144.57	166.80	6.63
0.075	14.32	13.22	5.52	99.44	85.19	6.34	162.57	192.13	6.70
0.1	19.22	15.75	5.60	118.20	103.62	6.43	190.51	238.38	6.79

[a] J_{theor} was calculated from Eq. 52. The estimated interfacial pH (pH_0) for each condition was determined from Eq. 51. Each J_{obs} value is the mean from at least two runs.

Table V—Comparison of the Observed (J_{obs}) and Theoretical (J_{theor}) Initial Dissolution Rates of 2-Naphthoic Acid from a Disk Rotating at 450 rpm into Varying Bulk Solution Concentrations of Morpholine Buffer at pH_{bulk} 8.00 and 8.50 (μ = 0.5 with Potassium Chloride and 25°) [a]

Total Bulk Solution Concentration of Morpholine, M	pH_{bulk} 8.00			pH_{bulk} 8.50		
	J_{obs}, moles/cm²/sec × 10^9	J_{theor}, moles/cm²/sec × 10^9	pH_0	J_{obs}, moles/cm²/sec × 10^9	J_{theor}, moles/cm²/sec × 10^9	pH_0
0.0	1.38	1.15	4.29	1.42	1.16	4.29
0.0001	—	1.17	4.30	—	1.23	4.33
0.0005	—	1.29	4.36	—	1.55	4.47
0.001	—	1.46	4.44	—	2.04	4.63
0.005	3.63	3.26	4.87	7.63	6.86	5.22
0.01	5.78	5.82	5.15	14.49	13.14	5.52
0.025	12.58	13.69	5.54	34.30	32.16	5.91
0.05	27.24	26.80	5.83	65.75	63.31	6.21
0.075	37.99	39.82	6.01	93.28	94.36	6.39
0.1	51.08	53.11	6.14	—	125.15	6.51

[a] J_{theor} was calculated from Eq. 52. The estimated interfacial pH (pH_0) for each condition was determined from Eq. 51. Each J_{obs} value is the mean from at least two determinations.

comparable concentrations of stronger bases in the bulk solution. Thus, intuitively, the basicity and acidity of the respective reacting buffer base and dissolving acid should be important in determining the initial dissolution rate, as evidenced by the presence of K_a^A and K_a^B in the coefficients of Eq. 51.

At constant pH_{bulk}, when the total buffer concentration in the bulk solution is increased, the maximum steady-state pH that can exist at the solid–liquid interface, pH_0, is that where pH_0 equals pH_{bulk}. This is confirmed by the data given in Table III for the acetate buffers at pH_{bulk} 4.50 and 5.00 since the calculated pH_0 values asymptotically approach the pH_{bulk} values as the total concentration of acetate buffer in the bulk solution rises.

The shape of the curves in Fig. 2 for the acetate buffers may be explained by the occurrence of a gradual change in controlling factors within the diffusion layer (which determine the 2-naphthoic acid dissolution rate) as the total bulk solution buffer concentration increases. When no buffer is present in the bulk solution and pH_{bulk} is maintained only by the pH-stat, the intrinsic solubility of the acid and its degree of dissociation at the solid–liquid interface determine the dissolution rate (1). The degree of dissociation is determined by reaction with water and hydroxide ion in the diffusion layer, as is the total flux (1).

Equation 52 expresses the total flux of the same acid when buffer is present in the bulk solution, and it includes an additional term to account for any buffer base species used up in the reaction with undissociated 2-naphthoic acid, hydrogen ion, or water in the diffusion layer. As the buffer base concentration increases, the corresponding term for its flux across the diffusion layer in Eq. 52 becomes more significant than the other terms. Despite a decrease in the flux terms in $[H^+]$ and $[OH^-]$ of Eq. 52 as the effective difference in pH across the diffusion layer diminishes, the asymptotic fluxes observed in Fig. 2 at pH_{bulk} 4.5 and 5.0 occur because there always is a finite difference between the buffer base concentration across the diffusion layer.

Eventually, the pH within the diffusion layer and pH_0 are controlled by the swamping effect of the buffer as it increases in concentration. Hence, the importance of the total buffer concentration in the bulk solution and the intrinsic solubility of the dissolving acid, $[HA]_0$, in determining the initial dissolution rate of that acid is seen.

The asymptotic fluxes were observed experimentally only with the acetate system at pH_{bulk} 4.50 and 5.0, because the corresponding pH_0 values in the absence of buffer did not differ greatly from asymptotic values they must approach (*i.e.*, pH_0 4.50 and 5.00) with increasing bulk solution acetate concentration. As observed in Table III, the relative increases in the dissolution rate in going from zero bulk solution acetate concentration to the asymptotic rate, given when pH_0 equals pH_{bulk}, were factors of 1.7 and 3.8 for pH_{bulk} 4.50 and 5.0, respectively. At pH_{bulk} 6.00, the total acetate concentration in the bulk solution must be much higher than that used experimentally for pH_0 to approach pH_{bulk}. Therefore, the asymptotic flux of 2-naphthoic acid is not observed at this pH_{bulk} value. It should be emphasized that the shapes of these curves are highly dependent on the intrinsic solubility of the dissolving acid since this factor determines the sensitivity of the total flux to changes in the total bulk solution buffer concentration.

Figures 3 and 4 and Tables IV and V report the observed and predicted dissolution rates of 2-naphthoic acid given by inclusion of imidazole and morpholine buffers in the bulk solution as a function of pH_{bulk} and buffer concentration. Similar explanations for the shapes of the curves to those given for the acetate system may be made, taking into consideration the greater basicity of these compounds and their diffusivities.

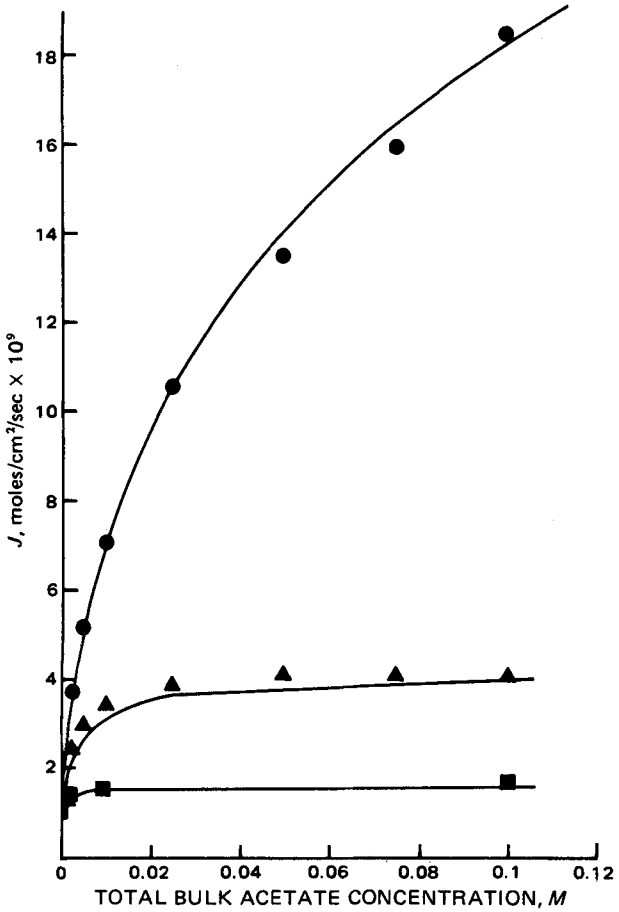

Figure 2—*Plot of the dissolution rate of 2-naphthoic acid from a solid disk rotating at 450 rpm into media of varying acetate buffer concentrations and pH_{bulk} [μ = 0.5 (potassium chloride) at 25°]. The pH_{bulk} was maintained constant by a pH-stat using 0.01 N NaOH. The solid continuous lines represent J_{theor}, and the symbols represent J_{obs} from Table III. Key: ■, pH_{bulk} 4.5; ▲, pH_{bulk} 5.0; and ●, pH_{bulk} 6.00.*

In view of the discussion of the shape of the plot of J *versus* buffer concentration in the bulk solution plot for pH_{bulk} 6.00 acetate buffer, considerable concentrations of imidazole and morpholine buffers at pH_{bulk} 6–8.5 are required in the bulk solution to make pH_0 at the 2-naphthoic solid–liquid interface equal to pH_{bulk}. Hence, over normal buffer concentration ranges, the asymptotic dissolution rate of 2-naphthoic acid was not seen for these buffers at the pH_{bulk} values studied.

To illustrate this point, consider the dissolution rate of 2-naphthoic acid at pH_{bulk} 8.00 in the absence of imidazole or morpholine buffer. The pH_0 (Tables IV and V) is 4.29, and the total concentration of 2-naphthoate at $X = 0$ under these conditions may be calculated readily. The same calculation may be performed at pH_0 8.00, the condition required for an asymptote, to give the corresponding total 2-naphthoate concentration at $X = 0$ when pH_0 and pH_{bulk} are equal. The ratio of the two total concentrations of 2-naphthoate calculated to exist at $X = 0$ directly represents the expected ratio of the dissolution rates under the same conditions. The ratio of the 2-naphthoic acid dissolution rate at pH_0 4.29 (zero buffer concentration) to that at pH_0 8.00 (asymptotic case) is ~3400. Hence, at pH_{bulk} 8.00, the asymptotic dissolution rate would be ~4.8×10^{-6} mole/cm²/sec, showing that a considerable imidazole or morpholine bulk solution concentration must be used to obtain this condition. The solubility and pKa of the acid also play an important role in determining the conditions at the solid–liquid interface and, therefore, also contribute in determining when the asymptotic dissolution rate is reached for given pH_{bulk} values and buffer solutions.

The curvature seen in the flux *versus* buffer concentration plots (Figs. 2–4) shows that linear extrapolation of the dissolution rate data *versus* buffer concentration plots obtained at high bulk solution buffer concentrations for a given pH_{bulk} is likely to give erroneous buffer-independent dissolution data. This method has been used frequently (18, 19)

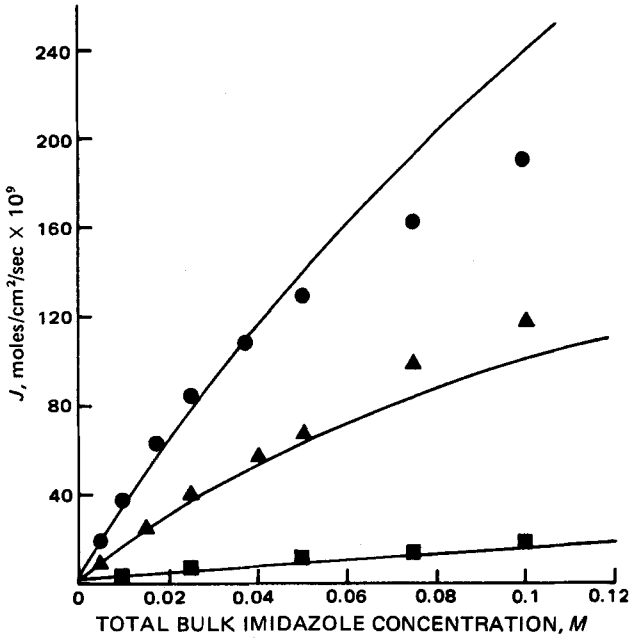

Figure 3—*Plot of the dissolution rate of 2-naphthoic acid from a solid disk rotating at 450 rpm into media of varying imidazole buffer concentration and pH_{bulk} [μ = 0.5 (potassium chloride) at 25°]. The pH_{bulk} was maintained constant by a pH-stat using 0.1 N NaOH. The solid continuous lines represent J_{theor}, and the symbols represent the data from Tables IV–VI. Key: ■, pH_{bulk} 6.00; ▲, pH_{bulk} 7.00; and ●, pH_{bulk} 8.00.*

to obtain buffer-independent dissolution rates where no pH-stat is employed and the buffer capacity of the buffer solutions is assumed to be large enough to resist changes in pH_{bulk} during a dissolution experiment. Referring to the imidazole data in Fig. 3, a linear least-squares fit of the four highest experimental imidazole concentrations at pH_{bulk} 8.00 gives an extrapolated J_0 value of ~6.4×10^{-8} mole/cm²/sec, whereas the true J_0 value (as determined by the pH-stat alone) is 1.4×10^{-9} moles/cm²/sec. Therefore, care should be taken in interpreting the intercept from extrapolated buffer dissolution data.

Dissolution rates also measured at the highest imidazole buffer concentration (0.1 M) without the pH-stat system operating, but otherwise

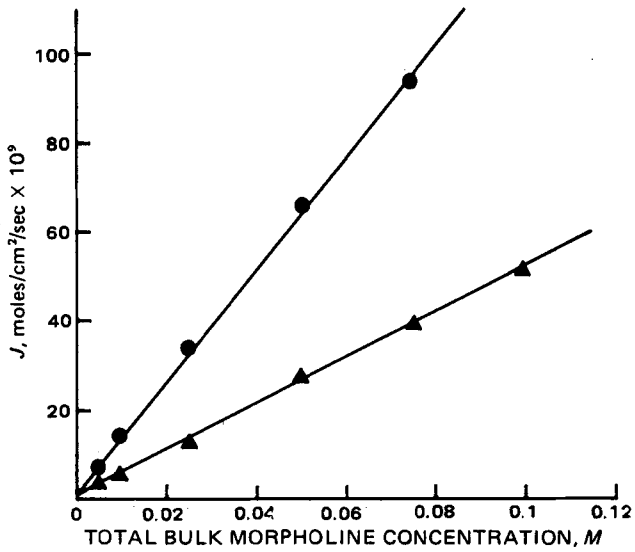

Figure 4—*Plot of the dissolution rate of 2-naphthoic acid from a solid disk rotating at 450 rpm into media of varying morpholine buffer concentration and pH_{bulk} [μ = 0.5 (potassium chloride) at 25°]. The pH_{bulk} was maintained constant by a pH-stat using 0.1 N NaOH. The solid continuous lines represent J_{theor}, and the symbols represent J_{obs} from Table VII. Key: ▲, pH_{bulk} 8.00; and ●, pH_{bulk} 8.50.*

Table VI—Concentration of Acetate Anion (Conjugate Buffer Base $[Ac^-]_h$) in the Bulk Solution and at the Solid–Liquid Interface ($[Ac^-]_0$) with Increasing Total Acetate Buffer Concentration at pH_{bulk} 6.0 and the Observed Flux (J_{obs}) of 2-Naphthoic Acid from a Disk Rotating at 450 rpm in pH-Statted Media (μ = 0.5 with Potassium Chloride and 25°)

Total Buffer Concentration of Acetate, *M*	$[Ac^-]_h$, moles/cm³ × 10⁷	$[Ac^-]_0$[a], moles/cm³ × 10⁷	$[Ac^-]_h - [Ac^-]_0$, moles/cm³ × 10⁷	Total Flux of 2-Naphthoic Acid (J_{obs}), moles/cm²/sec × 10⁹	pH_0[b]
0.0	0.0	0.0	0.0	1.33	4.28
0.001	9.62	5.70	3.92	—	4.72
0.0025	24.00	17.00	7.00	3.74	4.93
0.005	48.10	37.70	10.40	5.20	5.09
0.01	96.20	81.30	14.90	7.10	5.24
0.025	240.00	217.00	23.00	10.67	5.42
0.05	481.00	450.00	31.00	13.52	5.55
0.075	721.00	685.00	36.00	15.95	5.62
0.1	962.00	922.00	40.00	18.53	5.67

[a] Calculated from Eq. 50. [b] The pH_0 value is as defined in the text.

Table VII—Concentration of Free Imidazole Base ($[Im]_h$) in the Bulk Solution and at the Solid–Liquid Interface ($[Im]_0$) with Increasing Total Imidazole Bulk Solution Concentration at pH_{bulk} 6.0 and the Observed Flux (J_{obs}) of 2-Naphthoic Acid from a Disk Rotating at 450 rpm in a pH-Statted Aqueous Medium (μ = 0.5 with Potassium Chloride and 25°)

Total Buffer Concentration of Imidazole, *M*	$[Im]_h$, moles/cm³ × 10⁷	$[Im]_0$[a], moles/cm³ × 10⁷	$[Im]_h - [Im]_0$, moles/cm³ × 10⁷	Total Flux of 2-Naphthoic Acid (J_{obs}), moles/cm²/sec × 10⁹	pH_0[b]
0.0	0.0	0.0	0.0	1.33	4.28
0.01	6.33	0.46	5.87	3.02	4.83
0.025	15.80	2.43	13.37	6.01	5.16
0.05	31.70	8.33	23.37	10.07	5.40
0.075	47.50	16.50	31.00	13.21	5.52
0.10	63.30	26.20	37.10	15.75	5.60

[a] Calculated from Eq. 50. [b] The pH_0 value is as defined in the text.

as described previously at pH_{bulk} 7.00, did not differ significantly from those determined using the pH-stat with the same buffer solution. This finding was expected for solutions of high buffer capacity. However, in the non-pH-statted case, the pH_{bulk} decreases as the buffer capacity of the dissolution media is exceeded due to dissolution of the acid. If this point is reached during a dissolution run, sink conditions may cease to exist in the bulk solution and the dissolution rate could fall accordingly (20).

Influence of Basicity (K_a^B) of Buffer Base on Acid Dissolution Rate—Tables VI and VII list the concentration of acetate anion and imidazole free base, respectively, as a function of the total buffer concentration in the bulk solution at pH_{bulk} 6.0. They also list the corresponding buffer base concentrations at the solid–liquid interface (calculated from Eq. 50), the pH_0 (calculated from Eq. 51), the calculated buffer base concentration difference ($[B]_h - [B]_0$) across the diffusion layer, and the observed dissolution rate (J_{obs}) for 2-naphthoic acid. At a total buffer concentration of 0.01 *M* at pH_{bulk} 6.0 for acetate and imidazole, the concentrations of buffer base in the bulk solution differ by a factor of ~15, whereas the corresponding observed dissolution rates of 2-naphthoic acid differ by a factor of only ~2.5. If the comparison is extended further to 0.1 *M* total buffer concentration, the difference in the bulk solution buffer base concentration remains the same, but the observed dissolution rates become approximately equal, as do the pH_0 values.

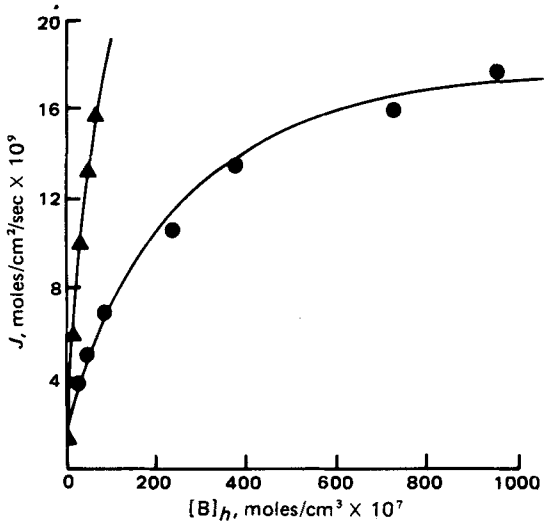

Figure 5—*Plot of 2-naphthoic acid dissolution rate (J)* versus *buffer base concentration in the bulk solution for acetate (●) and imidazole (▲) at pH_{bulk} 6.00. The data were taken from Tables VI and VII. The symbols represent J_{obs}, and the continuous line represents J_{theor} (given in Tables III and IV).*

These phenomena may be explained by the difference in the K_a^B value between the acetate anion and imidazole (a factor of ~400), assuming that their diffusivities are approximately equal. Figure 5 shows the predicted and observed dissolution rates for 2-naphthoic acid as a function of the bulk buffer base concentration at pH_{bulk} 6.00 for acetate and imidazole buffer solutions (taken from the data in Tables VI and VII). The effect of basicity in determining the extent of reaction with the dissolving acid and the proportion of buffer base in the bulk medium is observed clearly in Fig. 5 since imidazole has a much greater catalytic effect on the dissolution rate of 2-naphthoic acid for the same bulk solution buffer base concentration than does acetate. It also should be stressed that the intrinsic solubility of the dissolving acid and its K_a^A are important in determining such profiles since these parameters play a significant role in describing the conditions at the solid–liquid interface, as evidenced by their presence in the coefficients *r* and *s* of Eq. 51.

An alternative way of representing the effect of the buffer base con-

Table VIII—Regression and Correlation Data from Fig. 6 to Compute the Diffusivity (D_B) of the Acetate Anion and Imidazole Free Base in Aqueous Solution (μ = 0.5 with Potassium Chloride and 25°)

Buffer Solution at pH_{bulk} 6.00	Data from Fig. 6 (*J versus* $[B]_h - [B]_0$) Slope, cm/sec	Intercept, moles/cm²/sec	D_B, cm²/sec	*r*[a]
Acetate	4.3285×10^{-3}	6.3683×10^{-10}	8.61×10^{-6}	0.9962
Imidazole	4.0764×10^{-3}	5.86×10^{-10}	8.11×10^{-6}	0.9999

[a] Correlation coefficient.

Table IX—Recalculated Data from Higuchi *et al.* (7) for Benzoic Acid Dissolving into Solutions of Sodium Acetate (with 0.75 *M* NaCl) at 25° when No pH-Stat Was Used

Total Bulk Solution Concentration of Acetate, *M*	Calculated[a] from $\frac{[H^+]_h}{\sqrt{K_w K_a^B/m}}$, $M \times 10^9$	Calculated[a] pH_{bulk}	Calculated[b] pH_0	J_{obs}[c], moles/cm²/sec $\times 10^7$	J_{theor}[d], moles/cm²/sec $\times 10^7$
0.015	4.09	8.39	3.76	1.02	1.13
0.05	2.24	8.65	4.19	1.75	1.79
0.10	1.59	8.80	4.41	2.34	2.52
0.15	1.29	8.88	4.54	2.82	3.11
0.20	1.12	8.95	4.62	3.44	3.63
0.25	1.00	8.99	4.69	3.82	4.09

[a] Approximate hydrogen-ion concentration for the salt of a weak acid; K_w and K_a^B are used as in the text, m is the total concentration of the salt, and pH_{bulk} is calculated from $[H^+]_h$. [b] Calculated pH_0 assuming that pH-stat conditions are maintained in the bulk solution (Eq. 51 was used with parameters determined for benzoic acid from Ref. 1 and acetate from Tables I and II). [c] Calculated from data given in Ref. 7. [d] Theoretical value using an equivalent diffusion layer thickness, $h = 2.82 \times 10^{-3}$ cm (1).

centration in the bulk solution on the dissolution rate of 2-naphthoic acid is to plot J_{obs} *versus* $[B]_h - [B]_0$, the difference in the buffer base concentration across the diffusion layer created by the reaction therein. This plot is shown in Fig. 6 for the acetate and imidazole cases at pH_{bulk} 6.00. The relationship between J_{obs} and $[B]_h - [B]_0$ is approximately linear, as predicted by a modified form of Eq. 52:

$$J^{total} = \text{constant} + \frac{D_B}{h}([B]_h - [B]_0) \qquad \text{(Eq. 58)}$$

where the terms in [HA], $[H^+]$, and $[OH^-]$ represent a negligible contribution to the overall flux and may be grouped in the form of a constant. The slope of the plot of J *versus* $[B]_h - [B]_0$ is D_B/h, thus allowing D_B to be calculated if h is known. The regression and correlation data for the acetate and imidazole buffers from Fig. 6 are given in Table VIII together with the calculated values of D_B for both species in a solution with μ = 0.5 and at 25°. The D_B values thus derived are not obtained entirely from experiment since the calculation of $[B]_0$ requires some estimate of the values of D_B initially. However, close agreement is observed between assumed values (Table II) and derived values of D_B (Fig. 6). Thus, consistency between theory and experiment is obtained under the conditions described, suggesting that the assumed value of D_B is reasonable.

Higuchi *et al.* (7) used different bases in the dissolution media of benzoic acid in a similar study to that described here. They did not control the pH_{bulk} during the dissolution experiments apart from the natural buffer capacity exerted by the added bases. In the case of benzoic acid dissolving into solutions of varying sodium acetate concentration (with 0.75 *M* NaCl as the added electrolyte and a temperature of 25°), the dissolution rate was given as a function of the acetate concentration.

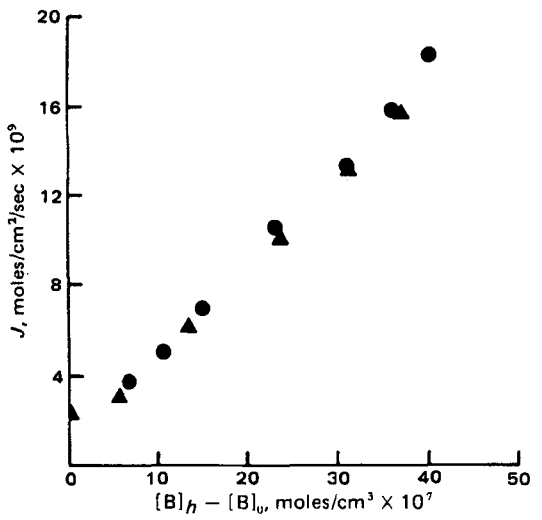

Figure 6—*Plot of 2-naphthoic acid dissolution rate (J)* versus *buffer base concentration difference ($[B]_h - [B]_0$) across the diffusion layer at steady state for acetate (●) and imidazole (▲) at pH_{bulk} 6.00. The data were taken from Tables VI and VII. The symbols represent observed rates (J_{obs}). Regression and correlation data are given in Table IX.*

Disregarding the differences in ionic strength between the two studies, a theoretical initial dissolution rate of benzoic acid may be calculated from the data and methods given in Table IX[6].

The agreement between the observed and predicted J values appears to be excellent. A simplified form of Eq. 52 was used by Higuchi *et al.* (7) to explain the resulting fluxes of benzoic acid in solutions of bases stronger than sodium acetate:

$$J^{total} = \frac{D_{HA}}{h}[HA]_0 + \frac{D_B}{h}[B]_h \qquad \text{(Eq. 59)}$$

Equation 59 assumes the total bulk solution buffer concentration to be equivalent to that of the base species, $[B]_h$. In the case of acetate, the equilibrium between the dissolving benzoic acid and the incoming buffer base does not favor the formation of benzoate anion as much as a similar bulk solution concentration of a stronger base, such as monohydrogen phosphate or borate. Since reaction occurs to a lesser extent with acetate ion, $[B]_h$ and $[B]_0$ are much closer in value than they would be for other stronger bases. Therefore, Eq. 58 should be used in this case rather than Eq. 59. Furthermore, Eq. 59 applies only in special cases, whereas Eqs. 52 and 58 are more general.

The reason Eq. 59 is a good approximation for the flux of benzoic acid when stronger bases than acetate anion are used is that benzoic acid is relatively water soluble (compared to 2-naphthoic acid) and maintains its pH microenvironment within the diffusion layer by the self-buffering mechanism proposed earlier (1), even when large concentrations of strong base are present in the bulk dissolution medium. As a result, for strong bases, $[B]_h$ will always be significantly greater than $[B]_0$, therefore rendering Eq. 59 applicable.

pH_{bulk} and Its Relevance to Dissolution Rates of Weak Acids—From the data presented here for monoprotic weak acid dissolution rates in aqueous media, there are few situations where pH_0 equals pH_{bulk}. This occurs only when the acid dissociation is suppressed in the diffusion layer, when the acid is highly water insoluble, or when a base is present in the dissolution medium at such a high concentration that it swamps and controls completely the pH of the diffusion layer. The importance of the buffer base concentration in the bulk solution and the basicity of the base on the dissolution rate of weak acids cannot be overemphasized. It is extremely important that the concentration and composition of the buffer medium be stipulated in recording the dissolution rates of acids since the pH of the medium is only one of the variables (and possibly a minor variable) controlling the dissolution rate.

Species Profiles and pH across Postulated Diffusion Layer—Figure 7 shows the idealized sections of the diffusion layer for dissolution of 2-naphthoic acid in imidazole solutions of varying concentration and pH. The fractional distance across the diffusion layer is given by X/h, and the fractional concentrations of HA, A^-, H^+, and OH^- are as defined previously (1). The fractional concentration of BH^+ is defined in a similar way to that of HA (normalized to $[BH^+]_0$), and that of B is defined in a similar way to the fractional concentration of OH^- (normalized to $[B]_h$). Only the B and BH^+ species are shown along with the diffusion layer pH[7].

The profiles of all species within the diffusion layer are calculated using

[6] Hydrodynamic equivalence is assumed between J_{obs} and J_{theor} using $h = 2.82 \times 10^{-3}$ cm, derived from benzoic acid solubility data in Ref. 6 and the D_{HA} value used in Ref. 1.

[7] A summary of the nonnormalized data for all species at several total bulk solution buffer concentrations and pH_{bulk} values using acetate, imidazole, and morpholine can be obtained from V. J. Stella.

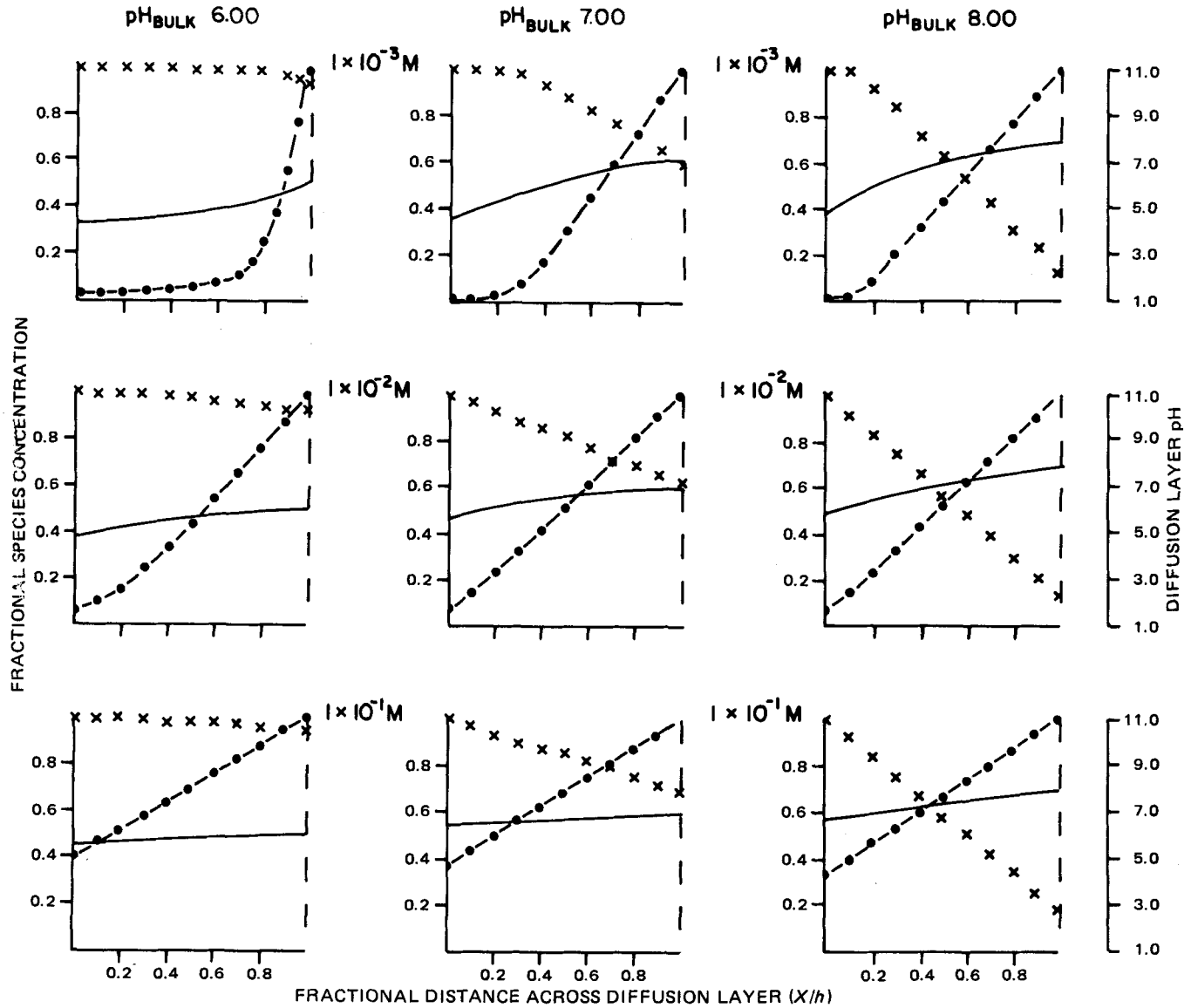

Figure 7—*Idealized sections across the postulated diffusion layer adjacent to the surface of dissolving 2-naphthoic acid. They depict the fractional concentration profiles of the imidazole buffer species and diffusion layer pH as a function of the changing pH_{bulk} and total buffer concentration in the bulk solution. Key: ×, imidazole conjugate acid, BH^+; - ●, imidazole base, B; and —, pH within the diffusion layer.*

Eq. 57 and a digital computer[1]. The fractional or normalized data are misleading as given in Fig. 7 and serve only as a comparison between the different conditions tested in the bulk solution. As the total buffer concentration in the bulk solution is increased at all pH_{bulk} values, the curvature in the diffusion layer pH profile becomes less pronounced since pH_0 approaches pH_{bulk}. Comparing the profiles obtained at pH_{bulk} 7.00 with imidazole buffer present in the dissolution medium to those obtained with 2-naphthoic acid when no buffer is present (see Fig. 10 in Ref. 1) at the same pH_{bulk}, the pH within the diffusion layer shows a much less abrupt change in the buffered case.

Many investigators have used the concept of a plane of reaction within the diffusion layer moving further toward or away from the solid–liquid boundary as the reactant concentration in the bulk solution is varied. This concept has been used to explain the dissolution of benzoic acid in sodium hydroxide solutions (21, 22), implying that the reaction decreases the effective film thickness and, therefore, catalyzes the dissolution rate. Where OH^- is the only base diffusing into the diffusion layer and reacting, the plane of reaction theory may be applied, as observed by the changing position in the film where an abrupt pH shift occurs when the bulk hydroxide-ion concentration is varied (1). However, this concept, as predicted by Higuchi *et al.* (7), does not apply very well to the buffered solution diffusion layers since no abrupt plane of reaction is observed due to lower reaction equilibrium constants between the acid and buffer bases than between the acid and hydroxide ion.

CONCLUSIONS

A method of determining the initial dissolution rate of a typical solid monoprotic weak acid in the presence of buffers is demonstrated. The bulk solution pH is controlled by the buffer in combination with a pH-stat. A theoretical model, using diffusion and simultaneous, instantaneous chemical reaction of the dissolving acid with the buffer base, hydroxide ion, and water within a postulated diffusion layer, accurately predicts the dissolution rate of the acid over a wide range of bulk solution buffer concentrations and pH values.

The dissolution of 2-naphthoic acid from a compressed disk of constant surface area at constant pH, ionic strength, and temperature in acetate, imidazole, and morpholine buffers as a function of the total bulk solution buffer concentration generally is nonlinear over a wide range of buffer concentrations. Furthermore, the total acid flux may asymptotically approach the limit where pH_0 equals pH_{bulk} with increasing total buffer concentration in the bulk solution. The approach to this condition is dependent on a complex function of the intrinsic solubility of the acid, the dissociation constants of the dissolving acid and the conjugate acid of the buffer base, the diffusivities of the reactants and products in the diffusion layer, the total concentration of the buffer in the bulk solution, and the pH of that solution.

In light of the results predicted by the model and the experimental results, the routine reporting of acid dissolution rates is meaningless

unless reference is made to the exact pH, buffer, and buffer concentrations used in the dissolution medium. Inclusion of the pKa of the buffer and acid, together with the intrinsic solubility of the acid, also is of use in interpretation of such dissolution data.

The relevance of the model presented here to the dissolution of acidic drugs from buffered tablet formulations is that, since the dissolution rate of an acidic drug is affected by the buffering effect and pH of its immediate surroundings, the incorporation of suitable buffering agents directly in tablet formulations should facilitate the release of the acidic drug from the tablet. The model certainly may assist the formulator in the choice of a buffering agent in the tablet relative to the pKa and solubility of the dissolving acid. However, direct application of the model to buffered dosage forms is difficult since the buffer must dissolve from the tablet simultaneously with the acidic drug. Furthermore, the surface area from which the dissolution occurs obviously changes during dissolution, and hydrodynamic conditions between an experiment and the *in vivo* situation are likely to differ markedly.

REFERENCES

(1) K. G. Mooney, M. A. Mintun, K. J. Himmelstein, and V. J. Stella, *J. Pharm. Sci.*, **70**, 13 (1981).

(2) G. Levy and B. Hayes, *N. Engl. J. Med.*, **262**, 1053 (1960).

(3) G. Levy, J. R. Leonards, and J. A. Procknal, *J. Pharm. Sci.*, **54**, 1719 (1965).

(4) V. Cotty, F. Zurzola, T. Beazley, and A. Rodgers, *ibid.*, **54**, 868 (1965).

(5) E. Nelson, *J. Am. Pharm. Assoc., Sci. Ed.*, **47**, 297 (1958).

(6) *Ibid.*, **47**, 300 (1958).

(7) W. I. Higuchi, E. L. Parrott, D. E. Wurster, and T. Higuchi, *J. Am. Pharm. Assoc., Sci. Ed.*, **47**, 376 (1958).

(8) W. I. Higuchi, E. Nelson, and J. Wagner, *J. Pharm. Sci.*, **53**, 333 (1964).

(9) V. Levich, "Physicochemical Hydrodynamics," Prentice-Hall, Englewood Cliffs, N.J., 1962.

(10) B. Carnahan, H. A. Luther, and J. O. Wilkes, "Applied Numerical Methods," Wiley, New York, N.Y., 1969, p. 171.

(11) J. N. Butler, "Ionic Equilibrium, A Mathematical Approach," Addison-Wesley, Reading, Mass., 1964.

(12) A. Albert and F. Sarjeant, "Ionization Constants of Acids and Bases," Meten & Co., London, England, 1962.

(13) G. Flynn, S. H. Yalkowsky, and T. J. Roseman, *J. Pharm. Sci.*, **63**, 479 (1974).

(14) V. Vitagliano and P. A. Lyons, *J. Am. Chem. Soc.*, **78**, 4538 (1956).

(15) W. J. Albery, A. R. Greenwood, and R. F. Kibble, *Trans. Faraday Soc.*, **63**, 360 (1967).

(16) J. M. Coulson and J. F. Richardson, "Chemical Engineering," 2nd ed., vol. 1, Pergamon, New York, N.Y., 1964, p. 306.

(17) T. Erdy-Gruz, "Transport Phenomena in Aqueous Solutions," Wiley, New York, N.Y., 1974.

(18) H. K. Lee, I. H. Pitman, and T. Higuchi, *Farm. Aikak.*, **80**, 55 (1971).

(19) H. K. Lee, H. Lambert, V. J. Stella, D. Wang, and T. Higuchi, *J. Pharm. Sci.*, **68**, 288 (1979).

(20) F. L. Underwood and D. E. Cadwallader, *ibid.*, **67**, 1163 (1978).

(21) C. V. King and S. S. Brodie, *J. Am. Chem. Soc.*, **49**, 1375 (1937).

(22) A. W. Hixson and S. J. Baum, *Ind. Eng. Chem.*, **36**, 528 (1944).

ACKNOWLEDGMENTS

Adapted in part from a dissertation submitted by K. G. Mooney to the University of Kansas in partial fulfillment of the Doctor of Philosophy degree requirements.

Supported by Grant GM22357 from the National Institutes of Health.

Pharmacokinetic Analysis by Linear System Approach I: Cimetidine Bioavailability and Second Peak Phenomenon

PETER VENG PEDERSEN

Received April 28, 1980, from the *Department of Pharmacy, School of Pharmacy, University of California, San Francisco, CA 94143.* Accepted for publication July 14, 1980.

Abstract □ The pharmacokinetics of cimetidine were evaluated using a linear system analysis that was formulated specifically to resolve the second peak in the blood drug concentration profile after oral dosing. The analysis exemplifies a new approach to pharmacokinetic modeling, which appears to be a valuable alternative to linear compartmental or physiological modeling. The formulation of linear system analysis according to a certain interpretation of a pharmacokinetic phenomenon avoids the complexity of conventional modeling, which often obscures the significance of the kinetic parameters. The new approach should result in a more rational analysis of pharmacokinetic phenomena because the less important pharmacokinetic processes are not specifically modeled but are still accounted for in the mathematical treatment. The bioavailability of cimetidine calculated by deconvolution agrees with previous findings. The model proposed to describe the second peak after oral absorption appears to agree well with the data and the hepatic recycling reported for cimetidine.

Keyphrases □ Linear system approach—evaluation of pharmacokinetics of cimetidine □ Pharmacokinetics—cimetidine, evaluation by linear system approach □ Cimetidine—evaluation of pharmacokinetics by linear system approach

Pharmacokinetic phenomena have been modeled and analyzed primarily according to two classes of models: linear compartmental models and physiological models. The classical linear compartmental models frequently provide a good fit to pharmacokinetic data. However, due to the fictitious structure of these models, which often bears little relation to the true nature of the pharmacokinetic processes, the parameters estimated from such models often have no real kinetic significance. The physiological models that attempt to be more realistic by considering such factors as blood flow and elimination and distribution in various organs and tissues may provide more meaningful results. However, the great number of physiological parameters and the difficulty of obtaining accurate and reliable estimates of these parameters make this approach very difficult. Both approaches to modeling

0022-3549/81/0100-0032$01.00/0

© 1981, American Pharmaceutical Association